Conformational Dynamics of Trialanine in Water: A Molecular Dynamics Study

Yuguang Mu and Gerhard Stock*

Institute of Physical and Theoretical Chemistry, J. W. Goethe University, Marie-Curie-Strasse 11, D-60439 Frankfurt, Germany

Received: October 30, 2001; In Final Form: January 3, 2002

Classical molecular dynamics (MD) studies of trialanine in aqueous solution are presented. The investigations have been inspired by recent 2D vibrational spectroscopy experiments of Woutersen and Hamm (*J. Phys. Chem. B* **2000**, *104*, 11316), who determined the structure and the conformational fluctuations of trialanine. The MD studies include various unbiased 20-ns simulations as well as umbrella sampling calculations of the potential of mean force along the central dihedral angles of trialanine. By employing the GROMOS96 force field, it is predicted that solvated trialanine is predominantly (∼80%) found in the extended conformations β and P_{II} and is also (∼16%) found in the helix conformation α_R. The results are explained by analyzing the free-energy contributions of intra- and intermolecular interactions, calculating the absolute entropy of the trialanine molecule, investigating the solvation and hydrogen bonding of the peptide, and studying the transitions between the extended and helix conformations. Moreover, the vibrational cross-relaxation rates associated with the two amide I modes of trialanine are calculated. The conformational structures and dynamics obtained from the MD studies are shown to be in good overall agreement with experimental data.

Introduction

The conformations available to a peptide in solution and the free-energy paths of its conformational transitions are of great importance to the folding and the function of the peptide. A theoretical description of the conformational dynamics of biomolecules can be obtained by classical molecular dynamics (MD) simulations, which allow us to investigate and understand biophysical processes in great microscopic detail.[1−7] Relying on the validity of the classical approximation and the accuracy of the force field employed, MD simulations still need to be validated by comparison to experimental data. Well-established experimental techniques such as nuclear magnetic resonance (NMR), for example, typically indicate the most important (i.e., most highly populated) conformations of a biomolecule.[8] However, most experiments provide time-averaged molecular structures and give only very limited information on the conformational dynamics.

A number of recent studies have shown that multidimensional nonlinear vibrational spectroscopy has the potential to reveal structural dynamics of biomolecules with picosecond or subpicosecond time resolution.[9−13] In particular, the secondary structure of small peptides has been studied by 2D vibrational spectroscopy of the amide I band, which mainly involves the C═O stretch of the peptide units. Similar to the cross-peaks in 2D NMR, the cross-peaks observed in the 2D vibrational spectrum of the amide I band reflect the coupling between the individual amide I oscillators along the peptide backbone. This coupling, which is primarily caused by the electrostatic interaction between the transition dipoles whose orientation depends on the (ϕ, ψ) dihedral angles of the peptides groups, directly monitors the structure of the peptide backbone. By using femtosecond infrared laser pulses, moreover, the delay time between the pulses can be employed to monitor the time dependence of the conformational dynamics.

Recently, Woutersen et al. have presented various 2D vibrational studies on trialanine (Ala_3) in aqueous solution.[12,13] The backbone structure of the peptide as well as its subpicosecond conformational dynamics were reported, and preliminary MD simulations showed good overall agreement with the experimental data. Trialanine represents an ideal model system for a joint experimental/theoretical investigation because it is among the simplest systems that exhibit typical features of biomolecules. For example, the backbone of the peptide exhibits several stable conformers that can be characterized by the central peptide dihedral angles ϕ and ψ (see Figure 1). In aqueous solution, trialanine forms hydrogen bonds with water, which are responsible for the stability of the conformers. In several aspects, trialanine is similar to alanine dipeptide ($CH_3CO-Ala-NHCH_3$), which has been employed as a benchmark problem for a number of theoretical descriptions.[14−21]

In this work, we present detailed computational studies on the structure and the dynamics of trialanine in water. Several 20-ns MD simulations as well as free-energy calculations of the potential of mean force along the central dihedral angles ϕ and ψ are reported. The contributions of intra- and intermolecular interactions to the free energies of the stable conformers are analyzed, the absolute entropy of the trialanine molecule is calculated, and the solvation and hydrogen bonding of the peptide are studied. Furthermore, the conformational transitions are discussed in some detail. Wherever possible, the theoretical results are compared to experimental data. We demonstrate that joint experimental/theoretical investigations may lead to a comprehensive picture of the conformational dynamics of a small peptide.

Computational Methods

MD Simulations. The MD simulations were performed with the GROMOS96 simulation program package employing the GROMOS force field 43A1.[22] Trialanine was placed in a periodic truncated octahedral box of simple point charge (SPC)

* Corresponding author. E-mail: stock@theochem.uni-frankfurt.de.

10.1021/jp013977e CCC: $22.00
Published on Web 04/18/2002

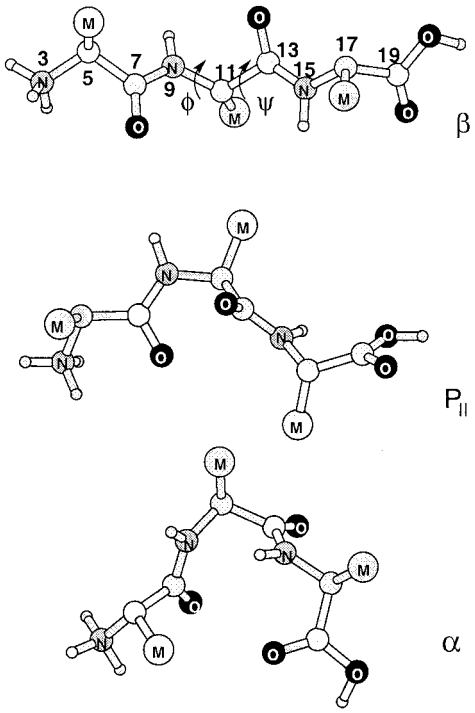

Figure 1. Snapshots of trialanine obtained from the MD simulation at 300 K showing three stable conformations: the extended conformations β at $(\phi, \psi) \approx (-120°, 130°)$ and P_{II} at $(\phi, \psi) \approx (-70°, 130°)$ as well as the helical conformation α_R at $(\phi, \psi) \approx (-70°, -40°)$. The first drawing also indicates the central dihedral angles ϕ and ψ and introduces the atom numbering used in this work.

water.[23] A minimum solute-to-wall distance of 1.5 nm was used, giving a total of 1263 water molecules. Assuming that the terminal groups are fully protonated to account for the experimental situation of pH = 1[12] and representing the $C_\alpha H$ and methyl groups as united atoms, the solute trialanine consists of 22 atoms (for atom numbering, see Figure 1).

The equation of motion was integrated by using a leapfrog algorithm with a time step of 2 fs. Covalent bond lengths were constrained by the procedure SHAKE with a relative geometric tolerance of 0.0001.[24] A twin-range cutoff of 0.8/1.4 nm was used for the nonbonded interactions, and a reaction-field correction with a permittivity of $\epsilon_{RF} = 54$ was employed.[5] The nonbonded interaction pair list was updated every 10 fs. The solute and solvent were weakly coupled to separate external temperature baths at 300 K.[25] The temperature coupling constant was 0.1 ps (0.01 during the first 10 ps). The total system was also weakly coupled to an external pressure bath at 1 atm using a coupling constant of 0.5 ps (0.05 during the first 10 ps).

Starting with a fully extended configuration of trialanine, the equilibration protocol consisted of 100 steps of steepest-descent minimization applied to the solvent molecules with a fixed solute, followed by a 5-ps MD simulation at 300 K of the solvent with fixed trialanine and another 5-ps simulation without constraining the position of trialanine. The simulation was then continued for 20 ns, during which time the coordinates were saved every 0.1 ps for analysis. An additional 20-ns simulation was performed at $T = 350$ K.

Potentials of Mean Force. One-dimensional potentials of mean force (PMF) along the central dihedral angles ϕ and ψ were calculated (i) directly from the unbiased MD simulation described above and (ii) by performing additional umbrella sampling simulations. In the former approach, the probability distribution $P(\phi)$ was obtained from a histogram of the MD data for $\phi(t)$ using a step size of 8°. The PMF along ϕ is then given by

$$\Delta G(\phi) = -k_B T[\ln P(\phi) - \ln P_{max}] \quad (1)$$

where P_{max} denotes the maximum of the distribution $P(\phi)$, which is subtracted to ensure that $\Delta G = 0$ for the lowest free-energy minimum.

In the umbrella sampling method, an auxiliary potential term $V_R(\phi) = k(\phi - \phi_0)^2$ is added to the Hamiltonian of the system, which restrains the sampling of ϕ around a given value ϕ_0.[26] By performing MD simulations including this potential, a biased probability distribution $P_R(\phi)$ is obtained, from which the unbiased PMF around ϕ_0 is given by

$$\Delta G(\phi) = k_B T \ln P_R(\phi) - V_R(\phi) + C \quad (2)$$

where $C = C(\phi_0)$ is a constant.[27] To obtain the overall PMF for trialanine in water, a force constant $k = 1$ kJ/(mol deg^2) was chosen, the restraint was changed in 10° increments, and a sampling window of 20° was used. Each restrained simulation was equilibrated for 25 000 steps and sampled for 100 000 steps to generate the PMF. The same procedures were used to calculate the PMF in ψ.

Entropy. To calculate the entropic contribution to the free energy, we use an approximate method recently proposed by Schlitter.[29] Assuming an N-particle system, he showed that an upper bound of the absolute entropy is given by

$$S = \frac{1}{2} k_B \ln \det\left\{\mathbf{1} + \frac{k_B T e^2}{\hbar^2}\mathbf{M}\sigma\right\} \quad (3)$$

Here **1** denotes the unit matrix, $e = \exp(1)$ is Euler's number, **M** is a diagonal matrix holding the masses of the system, and σ represents the covariance matrix of the atom-positional fluctuation with the elements

$$\sigma_{ij} = \langle (x_i - \langle x_i \rangle)(x_j - \langle x_j \rangle) \rangle \quad (4)$$

where $x_1,...,x_{3N}$ are the Cartesian coordinates of the N-particle system.

The derivation uses the assumptions that (i) every degree of freedom can be treated as a quantum-mechanical harmonic oscillator, the entropy of which is evaluated approximately, and that (ii) the frequency ω of each quantum harmonic oscillator can be calculated from the classical position variance $\langle x^2 \rangle_C$ by using the equipartition theorem $m\omega^2 \langle x^2 \rangle_C = k_B T$. Applying the method to a simple test system such as a Lennard-Jones fluid, it was found to predict the absolute entropy reliably with an accuracy of less than 10%.[30] Compared to a quasiharmonic analysis (which avoids the approximate calculation of the harmonic entropy[31]), Schlitter's ansatz was found to overestimate the absolute entropy of trialanine by ~6%, but the differences of the entropies (e.g., for helical and extended conformations) remained virtually unchanged.

As Cartesian coordinates are used in eq 3, the overall translational and rotational motions are included. For interpretational purposes (e.g., if the entropy difference between two conformations of a peptide is studied), one would like to consider only the entropy associated with the internal motions. Whereas the translation of the center of mass is readily removed, the overall rotation can only approximately be separated from the internal motion for a flexible molecule.[30] In the present calculation, we employed a least-squares fit to

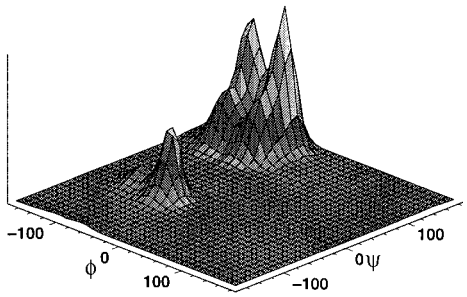

Figure 2. Ramachandran ϕ, ψ probability distribution of trialanine in water as obtained from the 20-ns simulation at 300 K.

TABLE 1: Conformations of Trialanine Sampled during the 20-ns Simulations at $T = 300$ and 350 K[a]

T(K)	state	ϕ(deg)	ψ(deg)	$\Delta\phi$(deg)	$\Delta\psi$(deg)	τ(ps)	P(%)
300	β	−122	130	17	24	8.5	42
	P_{II}	−67	132	15	22	8.1	41
	α_R	−76	−44	27	15	376	16
	α_L	41	86	23	69	9.5	0.8
350	β	−122	128	19	27	6.3	40
	P_{II}	−67	129	16	24	6.6	42
	α_R	−80	−46	32	19	83.8	14
	α_L	51	103	20	48	11.1	3.6

[a] For each conformer, the average dihedral angles ϕ and ψ and their RMS deviations $\Delta\phi$ and $\Delta\psi$ as well as the average lifetime τ and the population probability P are given.

superimpose the various structures obtained from the trajectory,[32] taking into account all 22 atoms of trialanine with mass weights.

In the studies reported below, we have restricted ourselves to the calculation of the entropy of the trialanine molecule. We did not attempt to compute the entropic contribution of the solvent because of the large dimension ($\sim 10^4$) of the corresponding covariance matrix and the long sampling times required.

Results and Discussion

Conformational Structures and Free Energies. To get a first impression of the conformations sampled by trialanine in aqueous solution, Figure 2 shows a Ramachandran representation of the probability distribution for the central dihedral angles (ϕ, ψ) obtained from the 20-ns simulation at 300 K. The map exhibits three distinct peaks that can be assigned to the right-handed helix conformation α_R located at (ϕ, ψ) $\approx$ (−70°, −40°) and two extended conformations, here referred to as β, [(ϕ, ψ) $\approx$ (−120°, 130°)], and P_{II}, [(ϕ, ψ) $\approx$ (−70°, 130°)]. The stereoviews of the three conformers are displayed in Figure 1. As shown by Figure 2, the GROMOS96 force-field description predicts that trialanine in water is predominantly ($\sim$80%) found in the extended conformations β and P_{II}. An additional MD simulation at higher temperature ($T = 350$ K) obtained a quite similar result, except that in this case there also exists a small population of the left-handed helix conformation α_L at (ϕ, ψ) $\approx$ (50°, 100°). For both simulations, the average values for (ϕ, ψ) and their RMS deviations as well as the population probability of each conformer are listed in Table 1.

To investigate to what extent the overall structure of trialanine depends on the other backbone dihedral angles, we have also studied the probability distribution of the terminal dihedral angles (i.e., ψ_N of the N terminal and ϕ_C of the C terminal). The ψ_N distribution exhibits a single maximum around 148° with a width of $\Delta\psi_N = 25.4°$. Compared to the central dihedral ψ, this peak corresponds to the extended conformers. Similar to the central dihedral ϕ, the ϕ_C distribution exhibits two peaks

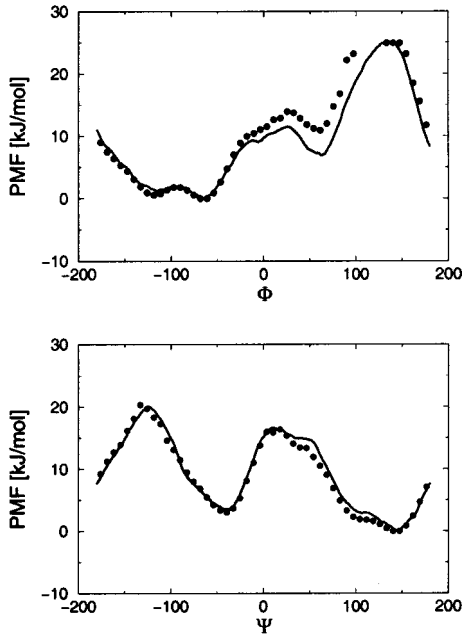

Figure 3. Potentials of mean force along the central dihedral angles ϕ and ψ of trialanine, obtained from the unbiased simulation (···) and the umbrella simulations (—full curves).

centered at $\sim$ −116° and −66°, respectively, with an overall width of $\Delta\psi_C = 41.42°$. Interestingly, both maxima are nearly equally sampled in the β, P_{II}, and α_R conformations. Hence, the overall conformation of trialanine is hardly affected by the terminal dihedrals.

To consider the relative free energies associated with the various conformations, Figure 3 shows the PMF in the coordinates ϕ and ψ obtained from the unbiased MD simulation (dotted lines) and from additional umbrella simulations (full lines). As is expected, for low energies, both calculations are in good agreement, but considerable deviations may occur in high-energy regions that are hardly sampled by the unbiased simulation. The PMF in ϕ exhibits two rather shallow minima of almost equal energy at −70° and −120°, corresponding to the β and P_{II} conformers, respectively. Furthermore, there is a minimum around $\phi = 50°$ associated with the left-handed α_L conformation, which is about 5 kJ/mol higher in energy. The transition between the helix conformation α_R and the extended conformations β and P_{II} is well described by the PMF in ψ. The barrier between the conformers is $\sim$17 kJ/mol. Compared to α_R, the extended conformations are lower in energy by almost 4 kJ/mol.

It is instructive to compare the PMF of trialanine with the corresponding free-energy curves of alanine dipeptide obtained for the same force field.[33] Generally speaking, the PMFs of both peptides are quite similar for both central dihedral angles ϕ and ψ. The main difference between the two systems is that the barrier in ψ between the helix and the extended conformations is about 4 kJ/mol lower in the case of alanine dipeptide. This finding and the associated shorter conformational lifetimes of alanine dipeptide are most likely explained by the smaller size of the dipeptide. The terminal groups of trialanine therefore effect a stabilization of the conformers.

It is interesting to investigate the origin of this free-energy difference between the helix and the extended conformations.[14,15] According to the thermodynamics relation

$$\Delta G = \Delta H - T\Delta S \tag{5}$$

the free-energy difference ΔG is caused by the changes of

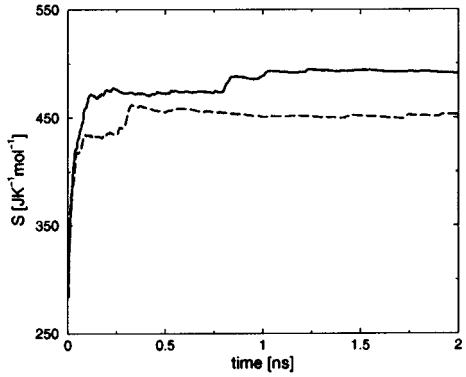

Figure 4. Absolute entropy of trialanine in the helical (---) and extended (—) conformations, respectively. The time evolution of the entropy reflects the phase-space exploration of the peptide.

TABLE 2: Contributions to the Free Energies of the Helix (α_R) and the Extended (β, P_{II}) Configurations[a]

	V^S_{bond}	V^S_{vdW}		$V^S_{el}V^{SB}_{vdW}$	V^{SB}_{el}	V_{tot}	$-TS$	ΔG
α_R	50.2	−15.6	−20.9	−39.6	−582.1	−607.8	−135.8	−743.6
β, P_{II}	49.1	−14.7	−42.9	−41.3	−546.0	−595.8	−147.2	−743.0
Δ	1.1	−0.9	22.0	1.7	−36.1	−12.0	11.4	−0.6

[a] Listed are the averages of the potential energies pertaining to the solute (superscript S), the solute−solvent interactions (superscript SB), and the entropic contribution to the free energy at $T = 300$ K. All energies are given in kJ/mol.

enthalpy ΔH and entropy ΔS, respectively. Let us first consider the entropic contribution to ΔG. Employing eq 3, the absolute entropy of trialanine has been calculated at times in which the molecule is exclusively in the helix or in the extended conformations. Figure 4 shows the time evolution of the entropy during such intervals. As the peptide explores new regions in phase space, the entropy initially exhibits a rapid increase. Within about a nanosecond, the phase-space exploration of the conformers has been completed, and the entropy fluctuates around a constant value. The entropic contribution to the free-energy difference is found to be $T\Delta S = 11.4$ kJ/mol (i.e., it clearly favors the extended conformers β and P_{II} over the helix conformer α_R). This finding is explained by the fact that the internal motion of an interconnected helix is more restricted than the internal motion of an extended conformation.

The change in enthalpy ΔH was obtained by averaging the solute−solute interaction energies V^S and the solute−solvent interaction energies V^{SB} separately for the helix and extended conformations. As listed in Table 2, the covalently bonded interaction energies V^S_{bond} as well as the nonbonded van der Waals energies V^S_{vdW} and V^{SB}_{vdW} differ very little for the two types of conformers. The main contribution to ΔH stems from the electrostatic interaction energies V^S_{el} and V^{SB}_{el}. Because of their large dipole moments, the α_R conformers show a strong electrostatic interaction with the polar water molecules and are therefore favored in energy by about $\Delta V^{SB}_{el} = -36$ kJ/mol. This energy gain is partly compensated by the solute−solute electrostatic interaction energy $\Delta V^S_{el} = 22$ kJ/mol, which reflects the strong Coulomb repulsions associated with the compact helix conformations.

Collectively, the solute−solute and solute−solvent interactions favor the α_R conformers by about $\Delta V_{tot} = -12$ kJ/mol. Subtracting the entropic contribution of 11.4 kJ/mol, the above analysis predicts that the helix and the extended conformations are virtually equal in free energy. Recalling that the PMF calculation yielded $\Delta G = 4$ kJ/mol, this finding indicates that there is a contribution of the solvent to the free-energy difference.[30] We note that the solvent contribution is again given as the difference between two large numbers (i.e., the entropy and the solvent−solvent interactions energy V^B).

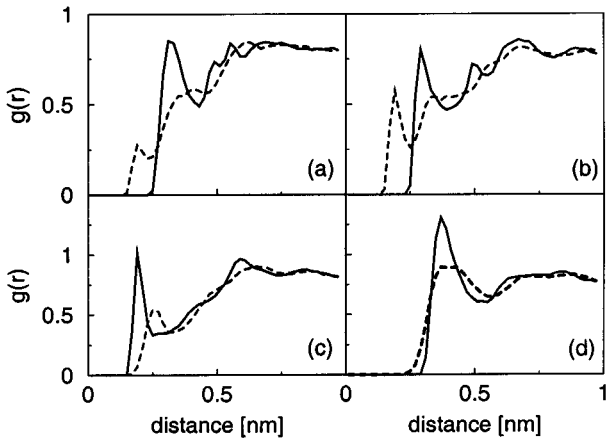

Figure 5. Radial distribution functions between the oxygen (—) or the hydrogen (---) of the solvent water and various sites of trialanine. (a) O8, (b) O14, (c) H10, and (d) M12.

Solvent Structure. The analysis above has shown that the main contribution to the solute−solvent interactions is of electrostatic origin, thus indicating the importance of hydrogen bonds between trialanine and water. To investigate the solvation of trialanine, we have considered the radial pair distribution functions $g(r)$ between various sites of trialanine and both the oxygen (Ow) and the hydrogen (Hw) of the surrounding water molecules. Apart from the differences between O8 and O14 discussed below, the distribution functions pertaining to analogous sites of trialanine turned out to be quite similar. Furthermore, there was only a small difference between the $g(r)$ in helix and extended conformations, reflecting the fact that V^{SB}_{el} is quite similar for both conformers.

As an example, Figure 5 shows the radial distribution functions $g(r)$ pertaining to the trialanine sites (a) O8, (b) O14, (c) H10, and (d) M12. In the case of the nonpolar methyl site M12, the radial distribution functions corresponding to Ow and Hw exhibit maxima at about the same position (i.e., there are similar probability distributions associated with either oxygen or hydrogen in the vicinity of the methyl group). Considering the polar sites O8, O14, and H10, on the other hand, there is a distinct shift of the first peak of $g(r)$ for Ow and Hw. The Ow atoms are closer to the positively charged site H10, but the Hw atoms are closer to the negatively charged site O14. The first minima of the radial distribution functions between O and Hw and between H and Ow clearly show the existence of hydrogen bonds between the polar sites of trialanine and neighboring water molecules.[20] A comparison of the distribution functions pertaining to the analogous sites O8 and O14 reveals that the first peak of the O8−Hw distribution functions is significantly smaller than that in the case of O14−Hw, thus indicating weaker hydrogen bonding of O8 because of the proximity of O8 to the NH_3^+ terminal, whose positive charge effects a considerable change in the solvation structure by repelling Hw and attracting Ow.

To obtain a more dynamical picture, the hydrogen bonding between trialanine and water has been monitored along the MD trajectory at 300 K. As a criterion for a hydrogen bond, we required a maximum proton acceptor distance of 0.25 nm and a minimum proton donor−acceptor angle of 125°.[22] To discard rapid large-amplitude fluctuations, moreover, only hydrogen bonds lasting longer than 2 ps have been considered in the statistics.[34] Table 3 shows the results for the average and

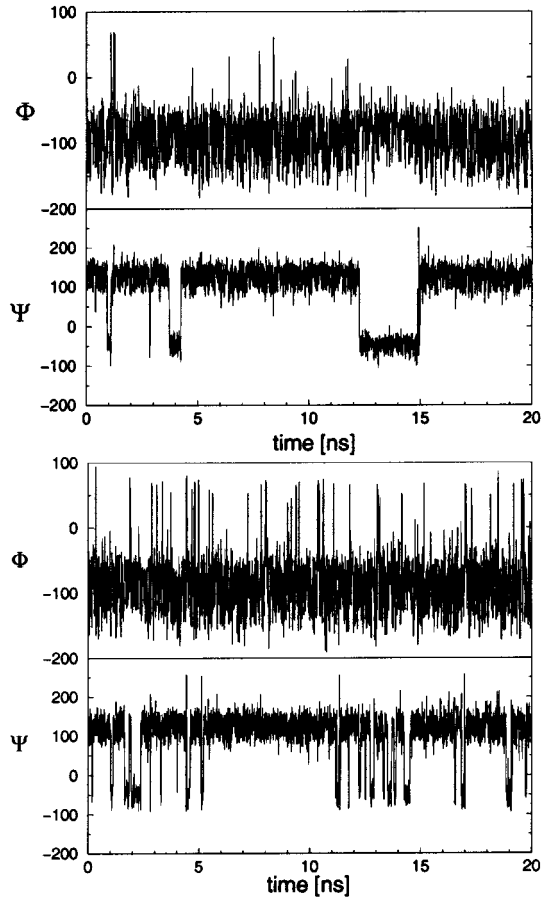

Figure 6. Time evolution of the two central dihedral angles ϕ and ψ of trialanine at 300 K (upper panel) and 350 K (lower panel).

TABLE 3: Average Lifetime τ_{av}, Maximal Lifetime τ_{max}, and Overall Probability of Hydrogen Bonding between Various Sites of Trialanine and Water

site	τ_{av}(ps)	τ_{max}(ps)	probability(%)
O8	3.4	7.2	25.0
O14	6.9	26.2	78.4
H10	8.6	46.1	86.4
H16	9.2	38.7	84.0

maximal lifetime and the overall probability of hydrogen bonding between various sites of trialanine and water. Roughly speaking, the polar sites of trialanine O14, H10, and H16 form intermolecular hydrogen bonds most of the time (~80%) and have an average lifetime of ~8 ps. As explained above, the probability and lifetime of hydrogen bonds involving the site O8 are significantly reduced because of the proximity of the charged NH_3^+ terminal group. Interestingly, hydrogen bonds including the amide hydrogen are found to be more stable and more likely to be formed than hydrogen bonds including carboxyl oxygens.

Conformational Dynamics. The PMFs discussed above point out the possibility of conformational transitions between the various stable conformers of trialanine. To study the dynamics of these transitions, Figure 6 shows the time evolution of the dihedral angles ϕ and ψ as obtained from the MD simulations at 300 and 350 K, respectively. Let us first discuss the time evolution of ψ, which accounts for conformational transitions between the helix conformation α_R and the extended conformations β and P_{II}. At room temperature (300 K), only four such transitions are observed within the 20-ns simulation time, but at 350 K, about twenty transitions are counted. Hence, the average lifetime of the α_R conformer is on the order of 400 ps at 300 K and 100 ps at 350 K, and the average lifetimes of the extended conformations (β and P_{II}) are estimated to be 2.5 ns at 300 K and 0.7 ns at 350 K. The population ratio of the two types of conformations, on the other hand, is virtually the same at both temperatures, $P_{hel}/P_{ext} \approx 0.18$. The value is in good agreement with the estimate obtained by the free-energy calculations, $\exp(-\Delta G/k_B T) = 0.19$.

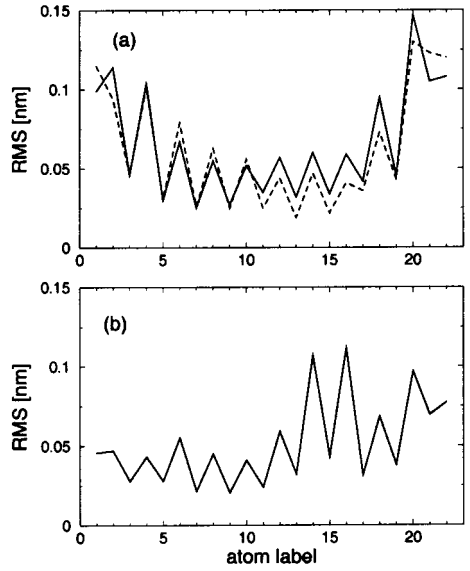

Figure 7. Root-mean-square positional fluctuations of the atoms of trialanine. Shown are (a) equilibrium fluctuations of the helix (---) and the extended (—solid line) conformations as well as (b) nonequilibrium fluctuations occurring during the transitions between the two conformers.

The time evolution of dihedral angles ϕ mainly reflects conformational transitions between the two extended conformers β and P_{II}. Because of the quite small barrier between these conformations, there are frequent transitions between β and P_{II}. The average lifetime of the two conformers is ~8 ps, which is virtually independent of temperature. Moreover, the dihedral angle ϕ monitors the formation of the left-handed helix conformer α_L. Although this state is hardly populated at room temperature, at 350 K, about 4% of trialanine molecules can be found in this conformation. Interestingly, the lifetime of α_L increases slightly at higher temperatures. Table 1 comprises the population probabilities and lifetimes of the conformers at both temperatures under consideration.

A measure of the fluctuations of the peptide is provided by the root-mean-square (RMS) deviations of the atomic positions plotted in Figure 7. In general, the backbone atoms of trialanine (labeled by odd numbers) are seen to undergo significantly smaller positional fluctuations than do the atoms of the side chain. The equilibrium fluctuations obtained for the helix conformation α_R and the two extended conformations β and P_{II} are quite similar. They differ mainly in the vicinity of the central peptide group, thus indicating that the motion of this peptide unit is more restricted in the helix conformation.

Figure 7 also compares the equilibrium fluctuations of trialanine (panel (a)) to the nonequilibrium fluctuations occurring during the transitions between the helix and extended conformations (panel (b)). While in equilibrium, the terminal atoms undergo much larger fluctuations than do the atoms of the central peptide group; this situation is reversed in the nonequilibrium case. In particular, one observes prominent fluctuations of the atoms O14 and H16, which indicate a quasi-rotational motion around the corresponding peptide bond during the conformational transition. A closer analysis of the trajectory reveals that most of the helix-extended transitions occur between the β

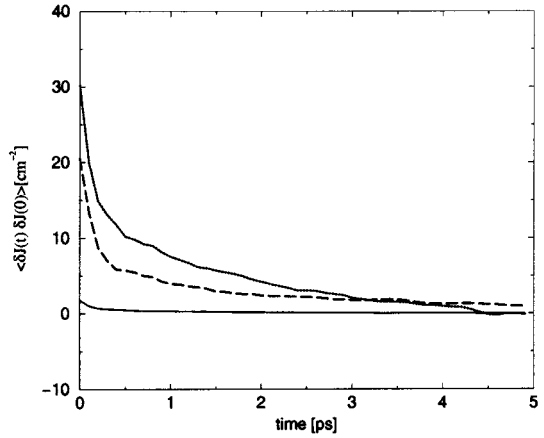

Figure 8. Autocorrelation function of the vibrational coupling fluctuations δJ between the two amide I oscillators of trialanine. Compared are results obtained for the three conformers β (---), P_{II} (—), and α_R (···) at 300 K.

conformer at (ϕ, ψ) $\approx$ (− 120°, 130°) and the side maximum of the α_R conformer located at (ϕ, ψ) $\approx$ (− 100°, − 40°). At first , this finding appears somewhat surprising because the stereoviews of trialanine shown in Figure 1 as well as the Ramachandran map shown in Figure 2 seem to suggest that there are transitions between α_R and the P_{II} conformation. However, the results are consistent with recent work showing that there may be several competing free-energy pathways between the extended and helical conformations[18] and that solvent motion is important for these transitions.[21]

Vibrational Cross-Relaxation. As mentioned in the Introduction, the conformational fluctuations of trialanine in water have recently been measured by femtosecond 2D vibrational spectroscopy of the amide I band.[13] In these experiments, the cross-peaks of the 2D spectrum reflect the coupling between the individual amide I oscillators along the peptide backbone. Upon excitation of a specific eigenstate of the amide I band, the time-resolved 2D vibrational spectrum may therefore monitor the cross-relaxation rate between a pair of eigenstates. In the weak-coupling limit, the vibrational cross-relaxation rate can be written as[36]

$$k = \frac{1}{\hbar^2}\int_{-\infty}^{\infty} \mathrm{d}t\, \mathrm{e}^{\mathrm{i}\Delta\epsilon t/\hbar}\langle \delta J(t)\delta J(0)\rangle \qquad (6)$$

where $\Delta\epsilon$ denotes the energy difference of the two eigenstates involved and $J(t) = J + \delta J(t)$ represents their instantaneous vibrational coupling. In the derivation of eq 6, the comparatively small effects due to vibrational dephasing have been neglected.[13]

To evaluate the coupling autocorrelation function $\langle \delta J(t)\delta J(0)\rangle$ from the MD simulations, we use ab initio calculations of Torri and Tasumi,[37] who computed the vibrational coupling J as a function of the two dihedral angles ϕ and ψ. Evaluating $J(t) = J[\phi(t),\psi(t)]$ along the MD trajectory,[38] the coupling autocorrelation functions obtained for the three conformers β, P_{II}, and α_R of trialanine are shown in Figure 8. The functions exhibit biexponential behavior

$$\langle \delta J(t)\delta J(0)\rangle = \delta J^2(w_1 \mathrm{e}^{-t/\tau_1} + w_2 \mathrm{e}^{-t/\tau_2}) \qquad (7)$$

where $\delta J^2 = \langle \delta J^2(0)\rangle$ denotes the amplitude of the fluctuations and τ_1, τ_2 are the correlation times with the weights w_1, w_2 ($w_1 + w_2 = 1$). Table 4 lists these quantities as obtained from the MD simulations at 300 and 350 K.

TABLE 4: Amplitude $\delta J^2 = \langle \delta J^2(0)\rangle$, Correlation Times τ_1, τ_2, and Weights w_1, w_2 of the Vibrational Coupling Autocorrelation Function $\langle \delta J(t)\delta J(0)\rangle$ Obtained from MD Simulations at 300 and 350 K

T(K)	state	$(\delta J)^2$(cm^{-2})	w_1	τ_1(ps)	w_2	τ_2(ps)
300	β	1.76	0.63	0.10	0.37	1.41
	P_{II}	30.2	0.51	0.10	0.49	1.53
	α_R	18.4	0.63	0.12	0.37	4.44
350	β	2.15	0.61	0.09	0.39	0.91
	P_{II}	37.61	0.50	0.11	0.50	1.08
	α_R	20.56	0.72	0.15	0.28	2.67

TABLE 5: Comparison of Computational and Experimental Results at $T = 300$ K Obtained for the Transition Dipole Angle Θ, the Mean Vibrational Coupling J, and the Cross-Relaxation Rate k at $\Delta\epsilon = 25$ and 70 cm^{-1}

state	Q(deg)	J(cm^{-1})	k_{25}(ns^{-1})	k_{70}(ns^{-1})
β	137	2.9	8	3
P_{II}	122	3.5	122	44
α_R	54	10.5	80	29
av	116	4.4	66	24
exp	106	6.0	190	70

The amplitude δJ^2 of the coupling fluctuations is seen to depend significantly on the conformational state of the peptide. In P_{II}, the fluctuations are about twice as large as those in α_R and more than 20 times larger than those in β. Because 2D vibrational spectroscopy directly measures these fluctuations, it is clear that the experiments are capable of monitoring conformational transition. The correlation times, on the other hand, are roughly similar for the three conformers. The short correlation time $\tau_1 \approx 100$ fs accounts for the inertial motion of the peptide, thus reflecting the mean free path length $\propto \sqrt{T}$. The larger correlation time $\tau_2 \approx 2$ ps reflects the diffusional motion of the peptide, which is expected to depend strongly on temperature. By increasing the temperature from 300 to 350 K, it is indeed found that τ_1 stays about the same, but τ_2 typically decreases.

To compare our result to experiment, eq 6 was employed to calculate the vibrational cross-relaxation rates at $\Delta\epsilon = 25$ and 70 cm^{-1}. These values of $\Delta\epsilon$ correspond to the energy difference of the two amide I peaks obtained for normal and ^{13}C isotope-labeled trialanine, respectively.[13] Comparing experimental and theoretical results collected in Table 5, we note that the calculated rates generally underestimate the experimental data. For example, the rates obtained by the conformational average are smaller by almost a factor of 3. It is clear, however, that the fluctuations obtained from the $J(\phi, \psi)$ map can represent only a lower bound of the true coupling because all fluctuations arising from the remaining coordinates are neglected in this approximation.

The situation looks different if one restricts the evaluation of the autocorrelation function to the sampling of the P_{II} conformation, which corresponds to the experimentally determined structure.[12] As this conformer gives rise to the largest fluctuations, in this case, there is excellent agreement (within 40%) between the rates obtained from theory and experiment. Apart from the vibrational cross-relaxation rates, the 2D vibrational experiments also measured the average vibrational coupling J and the angle Θ between the two amide I transition dipole vectors $\vec{\mu}$. As shown in Table 5, the experimental and computational results for these quantities are in quite good agreement.

Concluding Remarks

It is instructive to compare our studies of trialanine to various theoretical investigations of alanine dipeptide in water.[14−21] As

for trialanine, most studies on alanine dipeptide reported two types of stable conformations (extended and helical), which were located at similar positions in the (ϕ, ψ) plane. However, there is still the question of which conformer corresponds to the global minimum of the free-energy surface. Apart from technical details of the various calculations and methods, the discussion mainly arises from the insufficient accuracy of biomolecular force fields. Being typically twice as large as k_BT at room temperature, this accuracy introduces a considerable uncertainty into the calculation of the population probabilities of the conformations. As an alternative approach to the problem, one may perform high-level ab initio calculations for small peptides including a few solvent water molecules. On the basis of such a strategy, Han et al. recently compared calculated and experimental results for vibrational circular dichroism and Raman spectra and concluded that alanine dipeptide in water is predominantly found in a P_{II} conformation.[17] To compare to experimental data taken at room temperature, however, it is clear that the ab initio results have to be averaged with respect to the thermal fluctuations of the system, that is, a (often prohibitively) large number of computations are needed. Only very recently, the first attempts to conduct ab initio MD simulations of small peptides and proteins have been reported.[39,40]

Although there seems to be no unambiguous experimental data on the structure of alanine dipeptide, the 2D vibrational experiments of Woutersen and Hamm have indicated that trialanine in aqueous solution is mostly found in the P_{II} conformation.[12] This finding is confirmed by recent polarized visible Raman and FTIR experiments[41] as well as by preliminary data obtained from NMR investigations.[42] Within the uncertainties to be expected for a force-field calculation, the MD simulations reported in this work are in good agreement with this result, that is, roughly half of the population is predicted to be in the P_{II} conformation (see Table 1). Although it is clear that the force-field modeling exaggerates the population of the β conformer, the experimental data cannot rule out a small ($\lesssim$10%) population of the α_R conformation. Whether trialanine in water exhibits observable transitions between the α_R and P_{II} conformations as predicted by the MD simulations is therefore still an open question that is awaiting further theoretical and experimental investigations.

The MD studies on trialanine have revealed a microscopic picture of the structure and conformational dynamics of a small peptide in aqueous solution. For example, we have shown that the stabilization of a specific conformation of trialanine in water depends on the subtle interplay between the changes of enthalpy and entropy. The entropic contribution of the solute was found to favor the extended conformers β and P_{II} over the helix conformers α_R by about 11 kJ/mol, and the main contribution to the change in enthalpy was shown to arise from the electrostatic interactions that favor the α_R conformers by about 12 kJ/mol. As the difference in free energy between the helix and extended conformations was determined to be $\Delta G \approx 4$ kJ/mol, the calculations indicate a contribution of the solvent to the free-energy difference.

To make contact with the 2D vibrational experiments on trialanine in water, we have calculated the autocorrelation function of the vibrational coupling between the two amide I modes of trialanine. The Fourier transform of this function yields the corresponding cross-relaxation rates measured experimentally. Restricting the sampling of the coupling autocorrelation function to the experimentally confirmed P_{II} configuration, theoretical and experimental results for these rates were found to be in quite good agreement. Furthermore, a convincing match of theory and experiment was found for the average vibrational coupling J and the transition dipole angle Θ.

It is interesting to note that the evaluation of the coupling autocorrelation function at $T = 350$ K predicts a larger vibrational cross-relaxation rate for normal trialanine (i.e., at $\Delta\epsilon = 25$ cm^{-1}), but the rate remains roughly the same in the case of ^{13}C isotope-labeled trialanine (i.e., at $\Delta\epsilon = 75$ cm^{-1}) because in the latter case the rate is predominantly due to the inertial (i.e., short-time) component of the autocorrelation function that depends very little on temperature. At $\Delta\epsilon = 25$ cm^{-1}, on the other hand, the diffusional (i.e., long-time) component of the autocorrelation function, which strongly depends on temperature, becomes important. Preliminary experimental results[43] seem to confirm these theoretical observations.

The analysis given above indicates that a joint experimental/theoretical investigation may lead to a comprehensive understanding of the conformational dynamics of a small peptide in aqueous solution. To facilitate a more rigorous comparison of calculated and experimental data, further efforts and developments are required. Theoretical studies in our group include (i) investigations of the effects of various force fields, (ii) improved ab initio calculations of the vibrational couplings, and (iii) direct simulations of the time- and frequency-resolved 2D vibrational spectra. On the experimental side, further techniques to discriminate the various contributions to the complicated spectra are desirable (see, for example, ref 11). Compared to the experimental and theoretical methodology routinely used in NMR investigations, time-resolved multidimensional vibrational spectroscopy still holds great potential to be discovered.

Acknowledgment. We thank Peter Hamm and Rainer Hegger for many inspiring and illuminating discussions and Roland Bürgi, Tomas Hansson, and Wilfred van Gunsteren for helpful advice concerning the MD simulations. Financial support from the Deutsche Forschungsgemeinschaft and the Fonds der Chemischen Industrie is gratefully acknowledged.

References and Notes

(1) Allen, M. P.; Tildesley, D. J. *Computer Simulation of Liquids;* Oxford University Press: New York, 1987.

(2) McCammon, J. A.; Harvey, S. C. *Dynamics of Proteins and Nucleic Acids;* Cambridge University Press: New York, 1987.

(3) Leach, A. R. *Molecular Modeling;* Pearson Education Limited: London, 1996.

(4) Karplus, M. J.; Petsko, G. A. *Nature (London)* **1990**, *347*, 631.

(5) van Gunsteren, W. F.; Berendsen, H. J. C. *Angew. Chem., Int. Ed. Engl.* **1990**, *29*, 992.

(6) Kollman, P. A. *Chem. Rev.* **1993**, *93*, 2395.

(7) Brooks, C. L., III; Case, D. A. *Chem. Rev.* **1993**, *93*, 2487.

(8) Ernst, R. R.; Bodenhausen, G.; Wokaun, A. *Principles of Nuclear Magnetic Resonance in One and Two Dimensions;* Clarendon Press: Oxford, 1987.

(9) See, for example, papers in *Special Issue on Multidimensional Spectroscopies;* Mukamel, S., Hochstrasser, R. M., Eds.; *Chem. Phys.* **2001**, *266*.

(10) Hamm, P.; Lim, M.; Hochstrasser, R. M. *J. Phys. Chem. B* **1998**, *102*, 6123.

(11) Zanni, M. T.; Ge, N.-H.; Kim, Y. S.; Hochstrasser, R. M. *Proc. Natl. Acad. Sci. U.S.A.* **2001**, *98*, 11 265.

(12) Woutersen, S.; Hamm, P. *J. Phys. Chem. B* **2000**, *104*, 11316. Woutersen, S.; Hamm, P. *J. Chem. Phys.* **2001**, *114*, 2727.

(13) Woutersen, S.; Mu, Y.; Stock, G.; Hamm, P. *Proc. Natl. Acad. Sci. U.S.A.*. **2001**, *98*, 11 254.

(14) Pettitt, B. M.; Karplus, M. J. *J. Phys. Chem.* **1988**, *92*, 3994.

(15) Tobias, D. J.; Brooks, C. L., III *J. Phys. Chem.* **1992**, *96*, 3864.

(16) Cornell, W. D.; Gould, I. R.; Kollman, P. *J. Mol. Struct.* **1997**, *392*, 101.

(17) Han, W.-G.; Jalkanen, K. J.; Elstner, M.; Suhai, S. *J. Phys. Chem. B* **1998**, *102*, 2587.

(18) Apostolakis, J.; Ferrara, P.; Calfish, A. *J. Chem. Phys.* **1999**, *110*, 2099.
(19) Smith, P. E. *J. Chem. Phys.* **1999**, *111*, 5568.
(20) Kalko, S. G.; Guiàrdia, E.; Padró, J. A. *J. Phys. Chem. B* **1999**, *103*, 3935.
(21) Bolhuis, P. G.; Dellago, C.; Chandler, D. *Proc. Natl. Acad. Sci. U.S.A.* **2000**, *97*, 5877.
(22) van Gunsteren, W. F.; Billeter, S. R.; Eising, A. A.; Huenenberger, P. H.; Krueger, P.; Mark, A. E.; Scott, W. R. P.; Tirono, I. G. *Biomolecular Simulation: The GROMOS96 Manual and User Guide;* Vdf Hochschulverlage AG an der ETH Zürich: Zürich, 1996.
(23) Berendsen, H. J. C.; Postma, J. P. M.; van Gunsteren, W. F.; Hermans, J. In *Intermolecular Forces*; Pullman, B., Ed.; D. Reidel: Dordrecht, The Netherlands, 1981; p 331.
(24) Ryckaert, J. P.; Cicotti, G.; Berendsen, H. J. C. *J. Comput. Phys.* **1977**, *23*, 327.
(25) Berendsen, H. J. C.; Postma, J. P. M.; van Gunsteren, W. F.; Dinola, A.; Haak, J. R. *J. Chem. Phys.* **1984**, *81*, 3684.
(26) Chandler, D. *Introduction to Modern Statistical Mechanics;* Oxford University Press: Oxford, 1987.
(27) Similar to the weighted histogram analysis method,[28] the constant $C(\phi_i)$ pertaining to the *i*th sampling window is determined by a linear fit of the two adjacent free-energy functions $\Delta G(\phi, \phi_i)$ and $\Delta G(\phi, \phi_{i+1})$. The resulting loop error was smaller than 1 kJ/mol for both PMF calculations.
(28) Kumar, S.; Bouzida, J.; Swendsen, R.; Kollman, P.; Rosenberg, J. *J. Comput. Chem.* **1992**, *13*, 169.
(29) Schlitter, J. *Chem. Phys. Lett.* **1993**, *215*, 617.
(30) Schaefer, H.; Mark, A. E.; van Gunsteren, W. F. *J. Chem. Phys.* **2000**, *113*, 7809.
(31) Andricioaei, I.; Karplus, M. *J. Chem. Phys.* **2001**, *115*, 6289.
(32) McLachlan, A. D. *J. Mol. Biol.* **1979**, *128*, 49.
(33) Straatsma, T. P.; McCammon, J. A. *J. Chem. Phys.* **1994**, *101*, 5032.
(34) As discussed in ref 35, a time resolution of 2 ps appears appropriate because it is shorter than the rotational correlation time of SPC water (3.4 ps).
(35) Bonvin, A. M. J. J.; Sunnerhagen, M.; Otting, G.; van Gunsteren, W. F. *J. Mol. Biol.* **1998**, *282*, 859.
(36) Carrington, A.; McLachlan, A. D. *Introduction to Magnetic Resonance;* Harper & Row: New York, 1967.
(37) Torri, H.; Tasumi, M. *J. Raman Spectrosc.* **1998**, *29*, 81.
(38) The coupling autocorrelation function pertaining to a specific conformer was calculated through an ensemble average over all segments of the trajectory occupying the conformer for longer than $t = 20$ ps.
(39) Wei, D.; Guo, H.; Salahub, D. R. *Phys. Rev. E: Stat. Phys., Plasmas, Fluids, Relat. Interdiscip. Top.* **2001**, *64*, 011907.
(40) Liu, H.; Elstner, M.; Kaxiras, E.; Frauenstein, T.; Hermans, J.; Yang, W. *Proteins* **2001**, *44*, 484.
(41) Schweitzer-Stenner, R.; Eker, F.; Huang, Q.; Griebenow, K. *J. Am. Chem. Soc.* **2001**, *123*, 9628.
(42) Dorai, K.; Griesinger, C., to be submitted for publication.
(43) Woutersen, S.; Mu, Y.; Stock, G.; Hamm, P., to be submitted for publication.